Effects of Pressure and Nitrogen Dilution on Flame/Stretch Interactions of Laminar Premixed $H_2/O_2/N_2$ Flames

K. T. AUNG, M. I. HASSAN, AND G. M. FAETH*

Department of Aerospace Engineering, The University of Michigan, Ann Arbor, MI 48109-2118, U.S.A.

Effects of positive flame stretch on the laminar burning velocities of $H_2/O_2/N_2$ flames at normal temperatures and various pressures and nitrogen dilutions were studied both experimentally and computationally. Measurements and numerical simulations considered freely (outwardly)-propagating spherical laminar premixed flames at both stable and unstable preferential-diffusion conditions with fuel-equivalence ratios in the range 0.45–4.00, pressures in the range 0.35–4.00 atm, volumetric oxygen concentrations in the nonfuel gas in the range 0.125–0.210, and Karlovitz numbers in the range 0.0–0.6. For these conditions, both measured and predicted ratios of unstretched (plane flames) to stretched laminar burning velocities varied linearly with Karlovitz numbers, yielding Markstein numbers that were independent of Karlovitz numbers for a particular pressure and reactant mixture. Measured Markstein numbers were in the range −4 to 6, implying strong flame/stretch interactions. For hydrogen/air flames, the neutral preferential-diffusion condition shifted toward fuel-rich conditions with increasing pressure. Predictions of stretch-corrected laminar burning velocities and Markstein numbers, using typical contemporary chemical reaction mechanisms, were in reasonably good agreement with the measurements.

NOMENCLATURE

D	mass diffusivity
K	flame stretch
Ka	Karlovitz number, KD_u/S_L^2
L	Markstein length
Ma	Markstein number, L/δ_D
$O_2/(O_2 + N_2)$	fraction of O_2 (volume basis) in nonfuel gases
P	pressure
r_f	flame radius
S_L	laminar burning velocity based on unburned gas properties
$S'_{L\infty}$	value of S_L at largest radius observed
t	time
δ_D	characteristic flame thickness, D_u/S_L
ρ	density
ϕ	fuel-equivalence ratio

Subscripts

b	burned gas
max	maximum observed value
u	unburned gas
∞	asymptotic condition for an unstretched (plane flame)

INTRODUCTION

Recent measurements have shown that preferential-diffusion/stretch interactions of laminar premixed flames are large enough to affect the properties of strongly turbulent premixed flames in the thin flamelet regime, suggesting that these effects are important for most practical turbulent premixed flames [1, 2]. In addition, recent recognition of the strong effects of preferential-diffusion/stretch interactions of laminar premixed flames [3–14] also raises questions about past measurements of fundamental laminar burning velocities because practical laminar premixed flames in normal-gravity environments invariably are stretched to some extent. Finally, the sensitivity of laminar premixed flames to stretch, represented by the Markstein number [3–6], provides a new fundamental parameter that should be studied to better understand and model the properties of laminar premixed flames. Motivated by these considerations, the present study extends an earlier investigation of effects of flame stretch

* Corresponding author.

COMBUSTION AND FLAME 112:1–15 (1998)

Published by Elsevier Science Inc.

0010-2180/98/$19.00
PII S0010-2180(97)00010-2

on laminar premixed hydrogen/air flames at normal temperature and pressure (NTP) [6], to consider how this flame system is affected by varying pressure and nitrogen dilutions. Similar to past work in this laboratory [3–6], present measurements considered freely (outwardly)-propagating spherical laminar premixed flames in order to find laminar burning velocities as a function of flame stretch (represented by the Karlovitz number), the sensitivity of laminar burning velocities to flame stretch (represented by the Markstein number), and the fundamental laminar burning velocities of unstretched (plane) flames. The measurements were also used to evaluate corresponding numerical simulations of the experimentally-observed flames, based on detailed H_2/O_2 chemical reaction rate mechanisms due to Kim et al. [15], Wang and Rogg [16], Frenklach et al. [17], and Balakrishnan and Williams [18]. The following description of the study is brief, emphasizing the new experimental and computational findings at various pressures and nitrogen dilutions; Refs. 3–6 should be consulted for additional details about past findings and experimental and computational methods.

Present experimental and computational results were analyzed to find preferential-diffusion/stretch interactions the same way as earlier work in this laboratory for freely (outwardly)-propagating spherical laminar premixed flames [3–6]. In order to minimize problems of flame thickness variations, curvature and unsteadiness when interpreting preferential-diffusion/stretch interactions, flame conditions were limited to $\delta_D/r_f \ll 1$ [4, 6]. Effects of flame stretch on the laminar burning velocities were correlated using an early proposal of Markstein [19], after later generalization and extension at the limit of small stretch as discussed by Clavin [7], as follows [4, 6]:

$$S_L = S_{L\infty} - LK. \tag{1}$$

Present observations involve significant levels of stretch, therefore, Eq. 1 was extended using the "local conditions" hypothesis so that the flame response to effects of preferential-diffusion is represented by the characteristic length and time scales of stretched flames, δ_D and δ_D/S_L, rather than scales for the corresponding unstretched (plane flame) that can be very different. The diffusivity, D_u, used to find δ_D is arbitrary, as discussed in Ref. 6; therefore, the binary diffusivity of hydrogen with respect to nitrogen was used for D_u because this provides a conservative (large) estimate of δ_D when conditions having $\delta_D/r_f \ll 1$ were identified, similar to past work [1–4]. Introducing δ_D and δ_D/S_L into Eq. 1, the relationship between the laminar burning velocity and flame stretch becomes [3–6]:

$$S_{L\infty}/S_L = 1 + \mathrm{Ma}\,\mathrm{Ka}. \tag{2}$$

No linearity of either Eqs. 1 or 2, implying that values of L or Ma are independent of K or Ka for given unburned gas mixture properties, should be inferred (outside the asymptotic limit of small stretch); nevertheless, past observations generally find that Ma is independent of Ka for the accessible range of Ka where $\delta_D/r_f \ll 1$, which makes Fig. 2 particularly convenient for summarizing results outside the small stretch limit [3, 6]. The asymptotic form of Eq. 2 at the small stretch limit also is of interest because it has been used by some investigators [20, 21]; this equation can be found by expanding Eq. 2 in terms of S_L at the limit of small stretch (retaining only the leading terms) to yield [6]:

$$S_L/S_{L\infty} = 1 - \mathrm{Ma}_\infty\,\mathrm{Ka}_\infty, \tag{3}$$

which corresponds to the classical result from asymptotic theories [7], except for the trivial use of D_u in the definitions for Ma and Ka.

As discussed in Ref. 6, the present approach to characterize effects of flame stretch on laminar burning velocities through Eq. 2 is not unique but has several advantages for present use, pending the development of generally accepted methods to treat these interactions when $S_{L\infty}/S_L$ varies significantly from unity, as follows: the present results are found directly without the involvement of flame structure models that are difficult to completely define

and are likely to change as capabilities to predict flame structure improve; the present characterization of effects of stretch is concise which facilitates the use of the results by others; the positive and negative ranges of Ma provide a direct indication of stable and unstable flame surface conditions with respect to preferential-diffusion effects; and the present results can be readily transformed to provide direct comparisons with other methods for characterizing preferential-diffusion/stretch interactions. Nevertheless, the present approach has only been applied to freely (outwardly)-propagating spherical laminar premixed flames when $\delta_D/r_f \ll 1$ and effects of ignition disturbances and radiation are small (see [6] for discussion of the evaluation of effects of ignition disturbances and radiation). The limitations of this approach for more general preferential-diffusion/stretch interactions are not known so that other applications should be approached with caution.

Although others [10–12, 22–28] have measured effects of pressure and nitrogen dilution on the laminar burning velocities of $H_2/O_2/N_2$ flames, most earlier work did not consider effects of stretch on laminar burning velocities. An exception was Law and co-workers [10–12], who studied effects of flame stretch on hydrogen/air flames using an opposed-jet laminar premixed flame test configuration for fuel-lean conditions and pressures of 0.20–2.25 atm. Fundamental laminar burning velocities of unstretched (plane) flames were estimated from measurements at finite levels of stretch using an empirical extrapolation procedure, which represents the first attempt to apply stretch corrections to laminar burning velocities. Nevertheless, the pioneering work of Law and coworkers [10–12] should be extended, because their extrapolation scheme requires evaluation using alternative methods, and their results did not include information about flame sensitivity to stretch, i.e., Markstein numbers.

Earlier computational studies of effects of varying pressures and nitrogen dilutions on preferential-diffusion/stretch interactions of $H_2/O_2/N_2$ flames are limited to the work of Mishra et al. [20, 21]. These investigators used numerical simulations of freely-propagating spherical laminar premixed flames, considering conditions corresponding to the measurements of Kwon et al. [3] and Taylor and co-workers [13, 14], the latter results being confined to hydrogen/air flames at NTP. These calculations were based on the H_2/O_2 chemical reaction mechanism of Warnatz [29]. Good agreement between predictions and measurements was observed in some instances, however, the evaluation was limited to just a portion of the available measurements. Thus, a more complete assessment of the predictions and reaction kinetic models, considering variations of pressure and nitrogen dilution for $H_2/O_2/N_2$ flames, is needed.

In view of the current status of preferential-diffusion/stretch interactions of laminar premixed $H_2/O_2/N_2$ flames, the objectives of the present study were as follows: (1) to complete new measurements of outwardly-propagating spherical $H_2/O_2/N_2$ flames at various pressures and nitrogen dilutions; (2) to complete corresponding numerical simulations of the test flames; (3) to reduce both the measurements and the numerical simulations to find characteristic laminar flame properties ($S_{L\infty}$ and Ma); and (4) to compare the measurements and predictions with each other and with earlier results in the literature.

The discussion of the present study begins with descriptions of experimental and computational methods. Results are then discussed, considering burning velocity/stretch interactions, Markstein numbers, and unstretched laminar burning velocities, in turn.

EXPERIMENTAL METHODS

The present experiments were carried out in the spherical windowed chamber used during earlier work [6]. The reactant mixture was prepared within the chamber by adding gases at appropriate partial pressures to reach the desired initial pressure. The combustible mixture was spark-ignited at the center of the chamber, adjusting spark energies by trial so that they were close to the minimum ignition energy in order to control spark disturbances. Motion picture shadowgraphy was used to observe the motion of the flame surface as well as the

development of wrinkled surfaces due to effects of instabilities. Measurements of flame properties were limited to conditions where the surfaces were smooth; fortunately, the development of wrinkled surfaces due to preferential-diffusion and hydrodynamic instabilities was generally deferred to large enough radii so that at least some laminar burning velocity data could be obtained over the entire test range, see [6] for a discussion of flame surface wrinkling. Measurements were limited to flames having diameters less than 60 mm, which implies negligible pressure increases (less than 0.7%) within the chamber for the conditions of interest. In addition, earlier evaluations have shown that effects of motion in the burned gas and flow disturbances due to the presence of the chamber walls, were small [3].

Present measurements were limited to conditions where $\delta_D/r_f \leq 2\%$ which implies negligible curvature and transient effects associated with the thickness of the flame, as discussed by Tseng et al. [4]. In addition, rates of radiative heat losses were assumed to be negligible based on earlier estimates of these losses for hydrogen/air flames at NTP [6]. Finally, minimum flame radii were generally greater than 5 mm to avoid ignition disturbances and to satisfy the minimum δ_D/r_f criterion mentioned earlier, see [6] for a discussion of these limitations. For these conditions, Strehlow and Savage [30] show that the laminar burning velocity and stretch are given by the following quasi-steady expressions:

$$S_L = (\rho_b/\rho_u)\, dr_f/dt, \qquad K = (2/r_f)\, dr_f/dt. \tag{4}$$

Following past practice [3–6], S_L was found from Eq. 4 assuming adiabatic combustion at constant pressure with the reactant temperature equal to the initial temperature and with the same fuel-equivalence ratios in the unburned and burned gases. Then, the density ratio needed in Eq. 4 was found by assuming thermodynamic equilibrium in the combustion products for adiabatic, constant pressure and constant fuel-equivalence ratio combustion, using the CEC algorithm of Gordon and McBride [31] and the later STANJAN program of Reynolds [32]—both yielding essentially the same results. It should be noted, however, that this approach represents a *convention* which ignores preferential-diffusion effects that modify the local mixture fraction and thermal energy transport for stretched flames, and thus the local density ratio, ρ_b/ρ_u of the flames. This convention is convenient, however, because a single density ratio is used to relate flame speeds and laminar burning velocities for all levels of flame stretch which avoids current uncertainties about effects of flame stretch on the jump conditions across laminar premixed flames and corresponds to methods used during past studies [12–14, 20–28] which simplifies comparing present results with the findings of others. Once reliable information about jump conditions across stretched flames becomes available, current values of S_L can be updated with little difficulty. Fortunately, variations of flame properties due to variation of density ratios with stretch, estimated using the present numerical simulations of the flames, do not exceed 20% at the lowest pressure of 0.35 atm and 3% at the highest pressure of 4 atm. Naturally, these variations of density ratios with stretch do not affect the comparison between predicted and measured flame properties because both are treated the same way.

Final results were obtained by averaging the measurements of 4–6 tests at each flame condition considered. Estimation of the experimental uncertainties of the measurements is addressed in detail in Ref. 6. Experimental uncertainties (95% confidence) can be summarized as follows: S_L less than 9%; Ka less than 21%; S_{L^-} less than 12%; and Ma less than 25% for $|\mathrm{Ma}| > 1$, with uncertainties of Ma to increasing inversely proportional to |Ma| for $|\mathrm{Ma}| < 1$.

TEST CONDITIONS

Table 1 is a summary of test conditions and measured results for hydrogen/air flames at normal temperature, pressures of 0.35–4.00 atm and fuel-equivalence ratios of 0.45–4.00. It should be noted that some conditions listed in Table 1 exceed the limitation $\delta_D/r_f \leq 2\%$ due to the early appearance of flame wrinkling;

TABLE 1

Summary of Test Conditions for Hydrogen/Air Flames at Various Initial Pressures[a]

ϕ (−)	ρ_u/ρ_b (−)	$S'_{L,x}$ (mm/s)	$S_{L,x}$ (mm/s)	$\delta_{D,x}$ (μm)	K_{max} (s^{-1})	Ka_{max} (−)	Ma (−)
P = 0.35 atm (D_u = 208.3 mm^2/s)							
0.45[b]	4.75	760	640	320	2070	0.42	−1.4
0.75	6.20	1390	1370	150	3370	0.38	0.2
1.05	6.89	1790	1840	110	3770	0.34	0.8
1.40	6.64	2120	2270	90	4100	0.32	1.7
1.80	6.29	1980	2280	90	3540	0.36	2.8
2.20	5.95	1850	2100	100	2610	0.40	2.9
2.60	5.66	1660	1870	110	1950	0.54	3.0
3.00	5.39	1430	1700	120	1580	0.68	3.2
P = 0.50 atm (D_u = 145.8 mm^2/s)							
0.45[b]	4.75	630	680	210	1590	0.41	−0.2
0.75	6.20	1520	1550	90	2750	0.24	0.7
1.05	6.89	1910	2000	70	3980	0.27	1.5
1.40	6.66	2370	2490	60	5520	0.16	1.6
1.80	6.29	2180	2450	60	3260	0.31	3.5
2.20	5.95	2210	2380	60	4000	0.20	2.7
2.60	5.66	2010	2160	70	3250	0.21	2.9
3.00	5.39	1620	1840	80	1670	0.39	3.8
3.50	5.09	1450	1710	80	1170	0.46	3.7
4.00	4.82	1300	1470	100	1170	0.43	4.4
P = 1.0 atm (D_u = 72.9 mm^2/s)							
0.45[b]	4.75	470	500	150	4750	0.50	−1.1
0.75	6.22	1360	1340	50	2480	0.16	0.2
1.05	6.94	2030	2100	30	5680	0.15	1.7
1.40	6.68	2380	2520	30	5400	0.10	3.4
1.80	6.30	2490	2610	30	4330	0.08	3.7
2.20	5.96	2340	2460	30	3900	0.09	4.2
2.60	5.66	2060	2120	30	3580	0.09	3.9
3.00	5.39	1830	1930	40	2680	0.15	4.3
3.50	5.09	1570	1690	40	1830	0.18	4.8
4.00	4.82	1320	1410	50	1130	0.24	5.5
P = 2.00 atm (D_u = 36.5 mm^2/s)							
0.45[b]	4.75	470	380	100	1090	0.12	−2.7
0.75	6.23	1300	1250	30	3140	0.06	−0.4
1.05	6.99	2270	2090	20	5260	0.05	1.0
1.40	6.69	2730	2780	10	5810	0.01	1.5
1.80	6.31	2770	2830	10	6080	0.04	3.8
2.20	5.97	2740	2790	10	5390	0.01	3.9
2.60	5.66	2460	2500	10	4290	0.02	3.5
3.00	5.39	1920	2000	20	3210	0.04	4.0
3.50	5.09	1600	1670	20	2660	0.04	4.8
4.00	4.82	1160	1240	30	2190	0.05	5.1
P = 3.00 atm (D_u = 24.3 mm^2/s)							
0.45[b]	4.75	500	420	60	1050	0.10	−3.5
0.75	6.23	1410	1350	20	3330	0.04	−1.2
1.05	7.01	2120	2160	10	5800	0.03	1.1
1.40	6.70	2720	2790	10	6880	0.03	2.5
1.80	6.31	2880	2850	10	6490	0.02	2.6
2.20	5.97	2890	2740	10	5680	0.02	3.0
2.60	5.66	2380	2360	10	5530	0.02	2.1
3.00	5.39	2050	2080	10	3840	0.02	4.2
3.50	5.09	1560	1610	10	2870	0.03	3.8
4.00	4.82	1210	1260	20	1990	0.04	5.6

TABLE 1

(continued)

ϕ (−)	ρ_u/ρ_b (−)	$S'_{L\infty}$ (mm/s)	$S_{L\infty}$ (mm/s)	$\delta_{D\infty}$ (μm)	K_{max} (s^{-1})	Ka_{max} (−)	Ma (−)
P = 4.00 atm (D_u = 18.2 mm^2/s)							
0.45[b]	4.75	560	460	40	1080	0.06	−4.0
0.75	6.24	1450	1300	10	3490	0.03	−1.5
1.80	6.32	2830	2850	6	5530	0.01	1.9
2.20	5.97	2760	2790	6	5180	0.02	3.9
2.60	5.66	2710	2660	7	5120	0.02	4.1
3.00	5.39	1990	2020	10	3700	0.02	4.2
3.50	5.09	1980	2000	10	3410	0.02	4.5
4.00	4.82	1550	1560	10	2370	0.02	3.3

[a] Initial mixture temperature 298 ± 3 K.
[b] $\delta_D/r_f > 2\%$.

therefore, results at these conditions are provided only for informational purposes. The tabulation provides values of D_u and ρ_u/ρ_b used to reduce the data, as well as the resulting values of $S'_{L\infty}$, $S_{L\infty}$, $\delta_{D\infty}$, K_{max}, Ka_{max} and Ma. Values of $S'_{L\infty}$ were found at the largest radius where measurements were made while values of $S_{L\infty}$ were found by extrapolating the measurements of S_L to Ka → 0, as discussed later, similar to past work [3–6]. Differences between $S'_{L\infty}$ and $S_{L\infty}$, are representative of effects of stretch on the determination of laminar burning velocities that are not corrected for stretch, at least for typical outwardly-propagating spherical laminar premixed flames. The largest differences between $S'_{L\infty}$ and $S_{L\infty}$ occur near the extremes of the fuel-equivalence ratios, where the absolute values of Ma are the largest: e.g., 20% at ϕ = 0.45 and 15% at ϕ = 3.00 at a pressure of 0.35 atm. The characteristic flame thicknesses, $\delta_{D\infty}$, were in the range 6–320 μm (but only in the range 6–150 μm when $\delta_D/r_f \leq 2\%$). The maximum stretch values are in the range 1050–6880 s^{-1} with corresponding values of Ka_{max} of 0.01–0.68. These values are relatively small compared to Ka on the order of unity that are associated with extinction conditions [9], which is a natural consequence of avoiding large values of δ_D/r_f and conditions where effects of the spark disturbances are significant. Values of Ma vary in the range −4 to 6, with the large absolute values of Ma indicative of significant levels of preferential-diffusion/stretch interactions, even for the present modest values of Ka_{max}.

Table 2 is a summary of test conditions and measured results, in the same format as Table 1, for $H_2/O_2/N_2$ flames at NTP with $O_2/(O_2 + N_2)$ in the range 0.125–0.175 [see Table 1 for corresponding values at $O_2/(O_2 + N_2)$ = 0.210] and fuel-equivalence ratios of 0.45–4.00. Some entries here exceed conditions where $\delta_D/r_f \leq 2\%$, and some also involve excessive effects of buoyancy; results for these conditions are included for informational purposes only. The differences between $S'_{L\infty}$ and $S_{L\infty}$ also tend to be largest near the extremes of the fuel-equivalence ratios, where the absolute values of Ma are largest: e.g., 50% at ϕ = 0.60 and 10% at ϕ = 3.00 for $O_2/(O_2 + N_2)$ = 0.125. Values of $\delta_{D\infty}$ are in the range 30–450 μm (but only 30–160 μm for conditions where $\delta_D/r_f \leq 2\%$). The maximum stretch values are in the range 390–5680 s^{-1}, with corresponding values of Ka_{max} in the range 0.09–0.59 [including results at $O_2/(O_2 + N_2)$ = 0.210 from Table 1], which are relatively far from extinction conditions as discussed earlier. Corresponding values of Ma are comparable to Table 1, in the range −4 to 6.

COMPUTATIONAL METHODS

Description of Numerical Simulations

Simulations of the outwardly-propagating spherical laminar premixed flames were car-

TABLE 2

Summary of Test Conditions for $H_2/O_2/N_2$ Flames[a]

ϕ (−)	ρ_u/ρ_b (−)	S'_{Lc} (mm/s)	S_{Lc} (mm/s)	δ_{Dc} (μm)	K_{max} (s^{-1})	Ka_{max} (−)	Ma (−)
$H_2/O_2/N_2$ Flames (D_u = 72.9 mm^2/s)							
$O_2/(O_2 + N_2) = 0.125$							
0.60[b]	5.00	240	160	450	820	0.34	−2.9
0.80	4.92	510	450	160	1270	0.17	−2.4
1.00	5.56	770	770	100	2050	0.21	−0.6
1.20	5.44	1030	1000	70	3500	0.28	0.3
1.50	5.24	1140	1140	60	3230	0.28	1.0
1.80	5.07	1140	1160	60	2100	0.19	1.6
2.00	4.96	1090	1140	60	1990	0.26	2.2
2.20	4.86	1100	1120	70	1870	0.20	2.6
2.60	4.67	900	960	80	1310	0.26	2.9
3.00[c]	4.50	790	860	80	890	0.40	4.4
$O_2/(O_2 + N_2) = 0.150$							
0.50[b]	4.17	350	210	350	740	0.20	−4.0
0.67[b]	4.99	570	450	160	1230	0.14	−3.3
0.83	5.56	880	750	100	2230	0.14	−2.4
1.00	6.07	1120	1040	70	2550	0.13	−1.0
1.25	5.94	1450	1440	50	3500	0.18	0.2
1.50	5.72	1660	1690	40	3190	0.11	1.9
1.67	5.60	1610	1670	40	3300	0.14	2.2
1.83	5.49	1630	1690	40	2920	0.13	2.5
2.17	5.27	1570	1620	50	2710	0.11	2.2
2.50	5.08	1470	1490	50	2150	0.13	2.8
3.00	4.82	1210	1280	60	1720	0.18	3.7
3.50	4.59	960	1000	70	1100	0.30	4.1
4.00[c]	4.38	800	830	90	390	0.59	6.0
$O_2/(O_2 + N_2) = 0.175$							
0.60[b]	5.05	710	560	130	1500	0.15	−3.1
0.80	5.89	1350	1080	70	3740	0.15	−1.7
1.00	6.48	1560	1530	50	4670	0.12	−0.1
1.20	6.39	1900	1920	40	3700	0.09	1.3
1.50	6.13	2160	2210	30	4130	0.10	2.6
1.80	5.88	2080	2160	30	4030	0.10	2.8
2.00	5.73	1920	1980	40	4500	0.19	2.5
2.20	5.59	1870	1930	40	4310	0.19	2.9
2.60	5.32	1720	1800	40	3280	0.17	3.4
3.00	5.08	1510	1660	40	2430	0.17	4.1
3.50	4.82	1380	1440	50	2210	0.22	4.2
4.00[c]	4.59	1060	1190	60	860	0.34	5.8

[a] Initial mixture pressure and temperature 1 atm, and 298 ± 3 K.
[b] $\delta_D/r_f > 2\%$.
[c] Buoyant flame.

ried out using the unsteady, one-dimensional governing equations incorporated in the laminar flame computer code called RUN-1DL, due to Rogg [33]. This algorithm allows for mixture-averaged multicomponent diffusion, thermal diffusion, variable thermochemical properties and variable transport properties, which is a sufficiently accurate treatment of transport for present purposes, as discussed in Ref. 6. The CHEMKIN package [34–36] was used as a preprocessor to find the thermochemical and transport properties for RUN-1DL.

The numerical algorithm employs self-adaptive gridding to deal with regions where property gradients are large, with the present results based on an Euler extrapolation method; the RUN-1DL manual [33] should be consulted for details. The computational grid in space and time was varied to insure numerical accuracy within 1%, estimated by Richardson extrapolation of S_L. The numerically simulated results were analyzed similar to the measurements, basing the flame position on the point where the temperature was the average of the hot and cold boundaries, however, the convention used for flame position was not critical because $\delta_D/r_f \ll 1$. Other limitations of the analysis of the properties of outwardly-propagating spherical laminar premixed flames apply to the numerical simulations similar to the experiments. Finally, the sensitivities of various aspects of the chemical kinetic mechanisms for the unstretched laminar burning velocities were evaluated using the PREMIX and CHEMKIN packages, following Kee and co-workers [37, 38].

Chemical Reaction Mechanism

Present calculations directly considered three detailed chemical reaction mechanisms—Kim et al. [15], Wang and Rogg [16], and GRI-Mech 2.1 due to Frenklach et al. [17]. Justified by the earlier study of hydrogen/air flames [6], C/H/O (relevant due to low levels of CO_2 in air) and N/O chemistry were neglected and only the H/O chemistry portions of the mechanisms of Refs. 13–17 were considered during present work. Both forward and backward reactions were included for all three reaction mechanisms. Thermodynamic and transport properties were taken from data bases recommended by the developers of each reaction mechanism, see original sources for details. Finally, the complete predictions of unstretched laminar burning velocities due to Balakrishnan and Williams [18] were also compared with a portion of the present measurements.

RESULTS AND DISCUSSION

Burning Velocity/Stretch Interactions

Results for finite flame radii involve finite values of K so that at the largest r_f observed, $S'_{L\infty}$ still differs from the fundamental unstretched laminar burning velocity of a plane flame, $S_{L\infty}$. Thus, values of $S_{L\infty}$ were found through Eq. 2 by plotting $S'_{L\infty}/S_L$ as a function of Ka similar to earlier work [3–6]. This yielded a linear plot so that extrapolation to Ka = 0 gave $S'_{L\infty}/S_{L\infty}$ and thus $S_{L\infty}$. This procedure was used to find the values of $S_{L\infty}$ and the corresponding values of $\delta_{D\infty}$, summarized in Tables 1 and 2. Then given $S_{L\infty}$, plots of $S_{L\infty}/S_L$ as a function of Ka can be constructed for various values of ϕ as suggested by Eq. 2. A sample of such results for H_2/air flames at 0.5 atm with $\phi = 0.45$, 0.75, 1.40, 2.20, and 3.00, is illustrated in Fig. 1. Results at the other test conditions summarized in Table 1 and 2 are similar.

Results of both measurements and predictions illustrated in Fig. 1 exhibit the linear relationship between $S_{L\infty}/S_L$, and Ka, also observed in Refs. 3–6, that was exploited to find $S_{L\infty}$. In addition, the slope of these plots, which is equal to the Markstein number according to Eq. 2, clearly is independent of Ka over the range of the measurements (which involves Ka < 0.6). It should be recalled, however, that this range of Ka is not close to extinction conditions (where Ka would be on the order of unity, see Law [9]) where the response of the flames to stretch is likely to change. Even for this modest range of Ka, however, the variation of $S_{L\infty}/S_L$ due to effects of stretch is substantial, e.g., values of $S_{L\infty}/S_L$ are in the range 0.8–2.0 in Fig. 1.

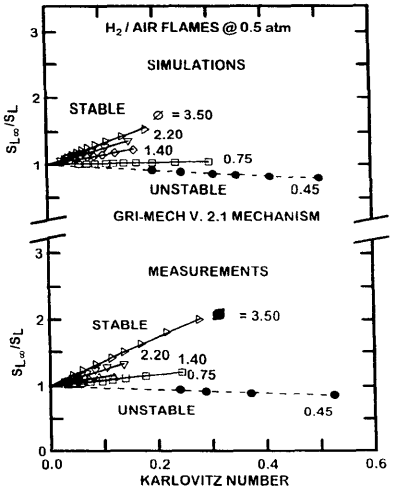

Fig. 1. Measured and predicted laminar burning velocities as a function of Karlovitz number and fuel-equivalence ratio for hydrogen/air flames at normal temperature and a pressure of 0.5 atm. Predictions based on the kinetics of Frenklach et al. [17].

Only the predicted variations of $S_{L\kappa}/S_L$ as a function of Ka, using the Frenklach et al. [17] mechanism, are shown in Fig. 1. Findings using the chemical reaction mechanisms of Kim et al. [15], and Wang and Rogg [16] are qualitatively similar (and will be quantified when measured and predicted Ma are discussed in the next section). The results of the simulations qualitatively agree with the measurements, however, evaluation of predicted preferential-diffusion/stretch properties are seen best from measured and predicted Markstein numbers, which are considered next.

Markstein Numbers

The slopes of the plots of $S_{L\kappa}/S_L$ as function of Ka yield the Markstein numbers, which were only a function of fuel-equivalence ratio for the present test conditions, similar to past work [3–6]. Measured and predicted (using the Kim et al. [15], Wang and Rogg [16], and Frenklach et al. [17] chemical reaction mechanisms) values of Ma for hydrogen/air flames at various pressures are plotted as a function of fuel-equivalence ratio in Figs. 2 and 3. The measured values of Ma vary from −4 to 6, highlighting the strong effects of stretch on hydrogen/air flames, with the largest absolute values of Ma occurring at very fuel-lean and fuel-rich conditions even through present conditions are far from quenching conditions. The neutral preferential-diffusion condition (Ma ≈ 0) shifts toward fuel-rich conditions with increasing pressure, confirming earlier observations of Kwon et al. [3] for $H_2/O_2/N_2$ flames at various N_2 concentrations and a pressure of 3 atm. For example, at 0.35 atm, Ma ≈ 0 oc-

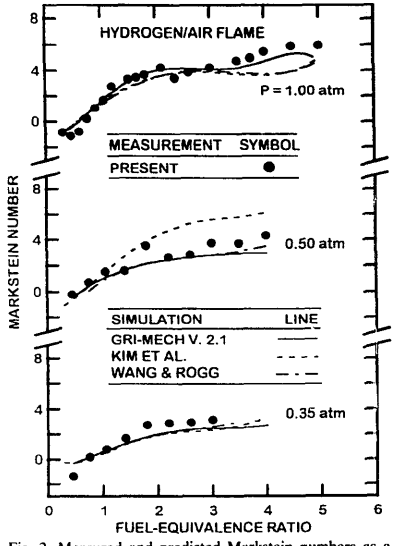

Fig. 2. Measured and predicted Markstein numbers as a function of fuel-equivalence ratio for hydrogen/air flames at normal temperature and pressures of 0.35, 0.50, and 1.00 atm. Measurements from the present study; predictions based on the kinetics of Kim et al. [15], Wang and Rogg [16], and Frenklach et al. [17].

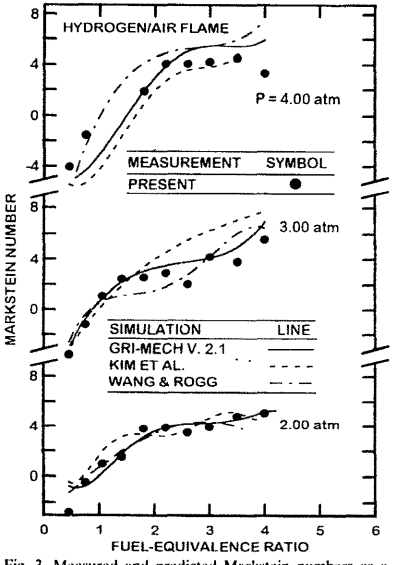

Fig. 3. Measured and predicted Markstein numbers as a function of fuel-equivalence ratio for hydrogen/air flames at normal temperature and pressures of 2.00, 3.00, and 4.00 atm. Measurements from the present study; predictions based on the kinetics of Kim [15], Wang and Rogg [16], and Frenklach et al. [17].

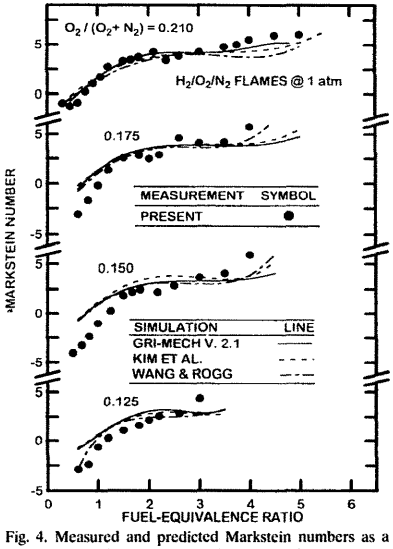

Fig. 4. Measured and predicted Markstein numbers as a function of fuel-equivalence ratio for $H_2/O_2/N_2$ flames at NTP with various nitrogen dilutions. Measurements from the present study; predictions based on the kinetics of Kim et al. [15], Wang and Rogg [16], and Frenklach et al. [17].

curs at $\phi \approx 0.6$ while at 4.0 atm, Ma ≈ 0 occurs at $\phi \approx 1.4$. The predicted results also exhibit a similar shift of the neutral preferential-diffusion condition with increasing pressure. The predicted Markstein numbers for all three reaction mechanisms are seen to be in good agreement with the measurements.

Measured and predicted (using the same mechanisms as Figs. 2 and 3) Markstein numbers for $H_2/O_2/N_2$ flames at NTP and various degrees of nitrogen dilution are plotted as a function of ϕ in Fig. 4. Measured Markstein numbers vary in the range -4 to 6, relatively independent of nitrogen dilution, highlighting the significant effects of stretch observed for these flames. Predicted Markstein numbers for all three reaction mechanisms are generally in reasonably good agreement with the measurements, with discrepancies between predictions and measurements being largest at very fuel-lean and fuel-rich conditions.

Unstretched Laminar Burning Velocities

Measured and predicted values of the laminar burning velocities of hydrogen/air flames at various pressures are plotted as a function of fuel-equivalence ratio in Figs. 5 and 6 for $P \leq 1$ and $P > 1$ atm, respectively. Measurements illustrated on the figures include results from Law [11], Fine [22], Grumer et al. [23], Iijima and Takeno [24], Manton and Milliken [25], and the present investigation, however, only the results of Law [11] and the present investigation are corrected for stretch. Even though the results of Fine [22] and Grumer et al. [23] are not corrected for stretch, they are in re-

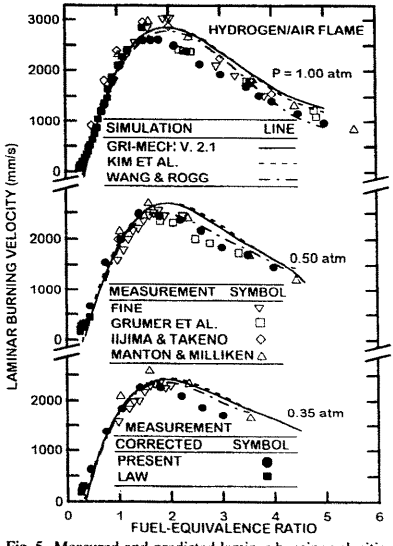

Fig. 5. Measured and predicted laminar burning velocities as a function of fuel-equivalence ratio for hydrogen/air flames at normal temperature and pressures of 0.35, 0.50, and 1.00 atm. Measurements from Fine [22], Grumer et al. [23], Iijima and Takeno [24], Law [11], Manton and Milliken [25], and the present study; predictions based on the kinetics of Kim et al. [15], Wang and Rogg [16], and Frenklach et al. [17].

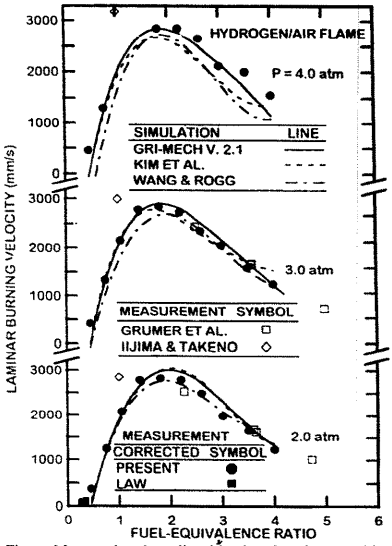

Fig. 6. Measured and predicted laminar burning velocities as a function of fuel-equivalence ratio for hydrogen/air flames at normal temperature and pressures of 2, 3, and 4 atm. Measurements from Grumer et al. [23], Iijima and Takeno [24], Law [11], and the present study; predictions based on the kinetics of Kim et al. [15], Wang and Rogg [16], and Frenklach et al. [17].

markably good agreement with the present stretch-corrected results. The predictions are based on the present numerical simulations using the Kim et al. [15], Wang and Rogg [16] and Frenklach et al. [17] chemical reaction mechanisms, as before. The measurements generally agree with the simulated results within experimental uncertainties for the present pressure range. A worrisome exception is fuel-lean conditions where predictions generally underestimate the measurements as the lean limit is approached; however, the discrepancies are most significant below the fuel-equivalence ratio range of the present measurements where effects of radiation, etc., not considered during the present computations, may be a factor. At elevated pressures, predicted results using the Frenklach et al. [17] mechanism are in remarkably good agreement with the present measurements; on the other hand, the results using the Wang and Rogg [16] mechanism agree better with the measurements at pressures of 0.5, 2.0, and 3.0 atm. The largest discrepancies between measurements and predictions within the range of the present experiments generally occur at fuel-rich conditions at low pressures, similar to earlier observations for hydrogen/air flames [6]. On the whole, however, the H_2/O_2 reaction mechanisms of Kim et al. [15], Wang and Rogg [16], and Frenklach et al. [17] may be satisfactory for many purposes, even though additional study and evaluation of the mechanisms and measurements at fuel-rich conditions, and possibly fuel-lean conditions near the limit, would be desirable.

Measured and predicted values of the laminar burning velocities of $H_2/O_2/N_2$ flames at NTP and various nitrogen dilutions are plotted as a function of fuel-equivalence ratio in Fig. 7. The measurements of Jahn [26], Mitani and Williams [27], and Takahashi et al. [28] at various nitrogen dilutions, none of which were corrected for stretch, are also shown on the plots. The present measurements and those of Jahn [26] and Mitani and Williams [27] are in very good agreement where they overlap, even though the latter measurements were not corrected for stretch. The measurements of Refs. 26 and 27 were obtained for conditions where stretch corrections might be expected; therefore, the agreement with present results is probably somewhat fortuitous. Present predictions based on the reaction mechanisms of Refs. 15–17 agree fairly well with present measurements at all values of $O_2/(O_2 + N_2)$. In contrast, the predictions of Balakrishnan and Williams [18] significantly overestimate the stretch-corrected results and were not considered any further. Finally, the somewhat larger discrepancies between the measurements and the predictions of Refs. 15–17 at fuel-rich conditions can be attributed to the greater effects of flame/stretch interactions, or larger Markstein numbers, that are present at these conditions.

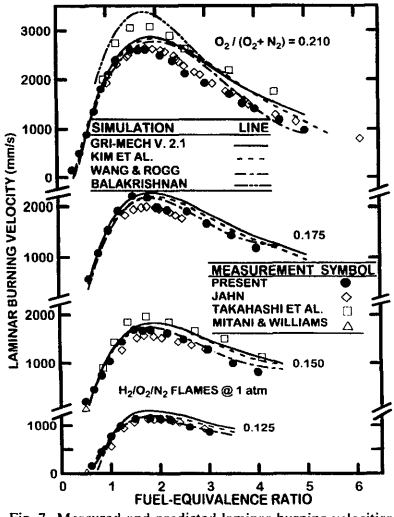

Fig. 7. Measured and predicted laminar burning velocities as a function of fuel-equivalence ratio for $H_2/O_2/N_2$ flames at NTP with various nitrogen dilutions. Measurements from Jahn [26], Mitani and Williams [27], Takahashi et al. [28], and the present study; present predictions based on the kinetics of Kim et al. [15], Wang and Rogg [16], and Frenklach et al. [17]; and earlier predictions due to Balakrishnan and Williams [18].

Sensitivity Analysis

In order to provide some insight about the most important chemical reactions needed to predict interactions between laminar burning velocities and stretch for hydrogen/air flames at low and high pressures, sensitivity calculations were carried out using the methods described by Kee et al. [37] and Grcar et al. [38]. These results are plotted in Figs. 8 and 9 for the pressure extremes of 0.35 and 4.00 atm, respectively. Normalized sensitivities are shown at ϕ = 0.45, 0.60, 1.80, and 3.50 for the ten reactions exhibiting the largest sensitivities based on the Frenklach et al. [17] mechanism; results for the Kim et al. [15] and Wang and Rogg [16] mechanisms were similar.

The reactions exhibiting the largest sensitivities at low and high pressures are similar, see Figs. 8 and 9; the chain propagation and branching reactions—$OH + H_2 = H + H_2O$, $H + HO_2 = OH + OH$, $H + O_2 = O + OH$ and $O + H_2 = OH + H$—exhibit the largest positive sensitivities while the recombination reactions—$OH + HO_2 = H_2O + O_2$, $H + HO_2 = H_2 + O_2$, and $H + O_2 + H_2O = HO_2 + H_2O$—exhibit the largest negative sensitivities, as expected. At high pressures, the sensitivities of the recombination reactions, particularly the reaction $H + O_2 + H_2O = HO_2 + H_2O$ become larger due to increased efficiency of H_2O as a third body. Among the reactions with large positive sensitivities, the reaction $OH + H_2 = H + H_2O$ shows a large increase in sensitivity with increasing pressure, suggesting that the competition between hydrogen

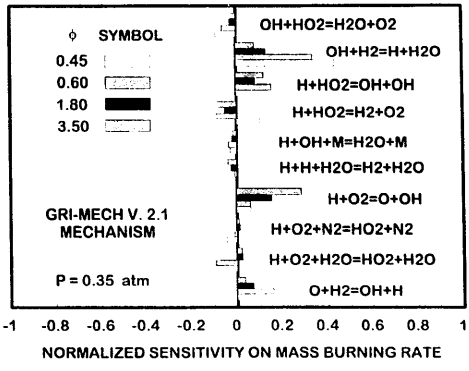

Fig. 8. Normalized sensitivities of kinetic parameters for the unstretched laminar burning velocities of hydrogen/air flames at normal temperature, a pressure of 0.35 atm and various fuel-equivalence ratios. Based on the kinetics of Frenklach et al. [17].

radical creation and destruction reactions are strongest for fuel-lean conditions at elevated pressures. Modifying reaction rate expressions to reduce discrepancies among the various measurements and predictions of both $S_{L\times}$ and Ma is a significant task, however, that is beyond the scope of the present investigation.

CONCLUSIONS

Effects of positive flame stretch on the laminar burning velocities observed in freely (outwardly)-propagating spherical laminar premixed flames involving $H_2/O_2/N_2$ mixtures at various pressures and nitrogen dilutions were studied both experimentally and computationally. The measurements involved outwardly-propagating spherical laminar premixed flames based on the methods similar to past work in this laboratory [3–6], while the computations involved numerical simulations of the same flame configuration considering the chemical reaction mechanisms of Kim et al. [15], Wang and Rogg [16], and Frenklach et al. [17], along with direct considerations of the laminar burning velocity predictions of Balakrishnan and Williams [18] for unstretched flames. Experiments were carried out at normal temperature and fuel-equivalence ratios in the range 0.45–4.00, pressures in the range 0.35–4.00 atm,

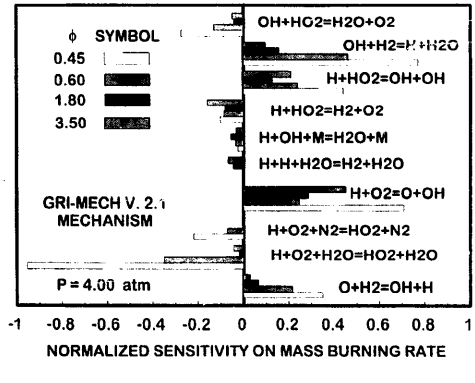

Fig. 9. Normalized sensitivities of kinetic parameters for the unstretched laminar burning velocities of hydrogen/air flames at normal temperature, a pressure of 4.00 atm and various fuel-equivalence ratios. Based on the kinetics of Frenklach et al. [17].

volumetric oxygen concentrations in the nonfuel gas in the range 0.125–0.210, Karlovitz numbers in the range 0.0–0.6 and laminar burning velocities in the range 100–3000 mm/s. The major conclusions of the study are as follows:

1. Effects of preferential-diffusion/stretch interactions for both the measurements and the predictions could be correlated according to $S_{L\infty}/S_L = 1 + \mathrm{Ma}\,\mathrm{Ka}$, where $S_{L\infty}/S_L$ varied linearly with Ka, yielding Markstein numbers that were only functions of reactant composition (fuel-equivalence ratios and nitrogen dilution) and pressure, similar to past work in this laboratory [3–6].
2. Effects of flame stretch on laminar burning velocities were substantial, yielding Markstein numbers in the range -4 to 6 with corresponding variations of $S_{L\infty}/S_L$ in the range 0.5–2.0; this behavior implies significant effects of flame stretch for typical laboratory measurements of laminar burning velocities as well as for the properties of turbulent premixed flames.
3. Predicted and measured unstretched laminar burning velocities and Markstein numbers exhibited encouraging agreement using the chemical reaction mechanisms of Kim et al. [15], Wang and Rogg [16], and Frenklach et al. [17]; nevertheless, discrepancies among the various predictions and measurements at fuel-rich conditions merit additional consideration. Predictions beyond the range of the present measurements, toward the lean limit, were also less satisfactory, perhaps due to effects not considered during the present simulations that become important at these conditions, e.g., radiation.
4. The neutral preferential-diffusion condition ($\mathrm{Ma} \approx 0$) was a function of pressure, shifting to fuel-rich conditions with increasing pressure, similar to earlier observations [3]. Values of Markstein numbers were relatively independent of nitrogen dilution, however, yielding the same range of Ma for all levels of nitrogen dilution considered during the present study.

This research was supported by the National Science Foundation Grant No. CTS-9321959, under the technical management of M. J. Linevsky and F. Fisher. Support from the Peace Fellowship Program of Egypt for one of us (M. I. Hassan) also is appreciated. L.-K. Tseng assisted with the initial phases of the research. Useful discussions with B. Rogg also are gratefully acknowledged.

REFERENCES

1. Wu, M.-S., Kwon, S., Driscoll, J. F., and Faeth, G. M., *Combust. Sci. Tech.* 78:69 (1991).
2. Law, C. K., and Faeth, G. M., *Prog. Energy Combust. Sci.* 20:65 (1994).
3. Kwon, S., Tseng, L.-K., and Faeth, G. M., *Combust. Flame* 90:230 (1992).
4. Tseng, L.-K., Ismail, M. A., and Faeth, G. M., *Combust. Flame* 95:410 (1993).
5. Aung, K. T., Tseng, L.-K., Ismail, M. A., and Faeth, G. M., *Combust. Flame* 102:526 (1995).
6. Aung, K. T., Hassan, M. A., and Faeth, G. M., *Combust. Flame*, in press.
7. Clavin, P., *Prog. Energy Combust. Sci.* 11:1 (1985).
8. Peters, N., *Twenty-First Symposium (International) on Combustion*, The Combustion Institute, Pittsburgh, 1986, p. 1231.
9. Law, C. K., *Twenty-Second Symposium (International) on Combustion*, The Combustion Institute, Pittsburgh, 1988, p. 1381.
10. Egolfopoulos, F. N., and Law, C. K., *Twenty-Third Symposium (International) on Combustion*, The Combustion Institute, Pittsburgh, 1990, p. 333.
11. Law, C. K., in *Reduced Kinetic Mechanisms for Applications in Combustion Systems* (N. Peters and B. Rogg, Eds.), Springer-Verlag, Berlin, 1993, p. 15.
12. Vagelopoulos, C. M., Egolfopoulos, F. N., and Law, C. K., *Twenty-Fifth Symposium (International) on Combustion*, The Combustion Institute, Pittsburgh, 1994, p. 1341.
13. Dowdy, D. R., Smith, D. B., Taylor, S. C., and Williams, A., *Twenty-Third Symposium (International) on Combustion*, The Combustion Institute, Pittsburgh, 1990, p. 325.
14. Taylor, S. C., Ph.D. Thesis, University of Leeds, 1991.
15. Kim, T. J., Yetter, R. A., and Dryer, F. L., *Twenty-Fifth Symposium (International) on Combustion*, The Combustion Institute, Pittsburgh, 1994, p. 759.
16. Wang, W., and Rogg, B., *Combust. Flame* 94:271 (1993).
17. Frenklach, M., Wang, H., Bowman, C. T., Hanson, R. K., Smith, G. P., Goldin, D. M., Gardiner, W. C., and Lissianski V., *Twenty-Fifth Symposium (International) on Combustion*, Work in Progress Poster 3-26, Irvine, California, 1994; also World Wide Web location http://www.gri.org/Basic Research/GRI-Mech, 1995.
18. Balakrishnan, G., and Williams, F. A., *J. Propulsion* 10:434 (1994).
19. Markstein, G. H., *Non-Steady Flame Propagation*, Pergamon, New York, 1964, p. 22.

20. Mishra, D. P., Paul, P. J., and Mukunda, H. S., *Combust. Flame* 97:35 (1994).
21. Mishra, D. P., Paul, P. J., and Mukunda, H. S., *Combust. Flame* 99:379 (1994).
22. Fine, B., "Stability Limits and Burning Velocities of Laminar Hydrogen-Air Flames at Reduced Pressures," Report No. NACA TN 3833, 1956.
23. Grumer, J., Cook, E. B., and Kubala, T. A., *Combust. Flame* 3:437 (1959).
24. Iijima, T., and Takeno, T., *Combust. Flame* 65:35 (1986).
25. Manton, J., and Milliken, B. B., *Proceedings of the Gas Dynamics Symposium on Aerothermochemistry*, Northwestern University Press, Evanston, 1956, p. 151.
26. Jahn, G., cited in Lewis, B. and von Elbe, G., *Combustion, Flames and Explosions of Gases*, 2nd ed., Academic, New York, 1961, p. 381.
27. Mitani, T., and Williams, F. A., *Combust. Flame* 39:169 (1980).
28. Takahashi, F., Mizomoto, M., and Ikai, S., *Alternative Energy Sources III* (T. N. Veziroglu, Ed.), Hemisphere Publishing Corp., Washington, D.C., 1983, p. 447.
29. Warnatz, J., in *Combustion Chemistry* (W. C. Gardiner, Jr., Ed.), Springer-Verlag, New York, 1984, p. 197.
30. Strehlow, R. A., and Savage, L. D., *Combust. Flame* 31:209 (1978).
31. Gordon, S., and McBride, B. J., "Computer Program for Calculation of Complex Chemical Equilibrium Compositions Rocket Performance, Incident and Reflected Shocks, and Chapman-Jouquet Detonations," Report No. NASA SP-273, 1971.
32. Reynolds, W. C., "The Element Potential Method for Chemical Equilibrium Analysis: Implementation in the Interactive Program STANJAN," Department of Mechanical Engineering Report, Stanford University, Stanford, CA, 1986.
33. Rogg, B., *RUN-1DL: The Cambridge Universal Laminar Flame Code*, Technical Report CUED/A-THERMO/TR39, Department of Engineering, University of Cambridge, 1991.
34. Kee, R. J., Rupley, F. M., and Miller, J. A., *CHEMKIN II: A Fortran Chemical Kinetics Package for the Analysis of Gas Phase Chemical Kinetics*, Report No. SAND89-8009B, Sandia National Laboratories, 1991.
35. Kee, R. J., Rupley, F. M., and Miller, J. A., *The CHEMKIN Thermodynamic Data Base*, Report No. SAND87-8215B, Sandia National Laboratories, 1990.
36. Kee, R. J., Dixon-Lewis, G., Warnatz, J., Coltrin, M. E., and Miller, J. A., *A FORTRAN Computer Code Package for the Evaluation of Gas-Phase, Multicomponent Transport Properties*, Report No. SAND86-8246, Sandia National Laboratories, 1986.
37. Kee, R. J., Grcar, J. F., Smooke, M. D., and Miller, J. A., *A Fortran Program for Modeling Steady Laminar One-Dimensional Premixed Flames*, Report No. SAND85-8240, Sandia National Laboratories, 1993.
38. Grcar, J. F., Kee, R. J., Smooke, M. D., and Miller, J. A., *Twenty-First Symposium (International) on Combustion*, The Combustion Institute, Pittsburgh, 1986, p. 1773.

Received August 12, 1996; accepted February 12, 1997